Eur. J. Mech. B/Fluids
© Elsevier, Paris

A NON-PERIODIC SPECTRAL METHOD WITH APPLICATION TO NONLINEAR WATER WAVES

Yehuda Agnon[1] and Harry B. Bingham[2]

[1]: *Coastal and Marine Engineering Research Institute, Department of Civil Engineering, Technion, Haifa 32000, Israel*
[2]: *Dept. of Mathematical Modelling, Technical University of Denmark, Building 21/305 Lyngby 2800, Denmark*

(Received 20 September 1998, revised and accepted 15 January 1999)

Abstract – Spectral methods are very efficient and powerful for solving periodic problems. A new spectral method is developed for problems with no spatial periodicity, and demonstrated for water waves. The method splits the potential into the sum of a prescribed non-periodic component and an unknown periodic component. Computed results are compared with experiments by Shemer *et al* (1998). © Elsevier, Paris

1. Introduction

Pseudo-spectral methods utilize the computational efficiency of the FFT algorithm to solve differential and pseudo-differential equations in spatially periodic domains. Here we use the case of water waves to introduce a method for applying these methods to non-periodic situations. Computing the nonlinear propagation of dispersive waves over a bathymetry and around vessels is required in many studies of coastal and offshore applications. Realistic problems pose a challenge to existing methods. In solving irrotational flow problems, the velocity potential can be expanded in terms of a set of basis functions which individually satisfy the Laplace equation. The coefficients of the series are then determined such that the sum satisfies the boundary conditions. The number of degrees of freedom, which typically corresponds to a set of values of the function (or its derivatives) at boundary points is much smaller than the number of points that would be required if the fluid volume was discretized. This corresponds to the lower dimension of the boundary. The basis functions can be polynomials, such as used in Boussinesq and high-order Boussinesq equations (Madsen and Schäffer, 1998). They can be singular Green's functions, such as used in boundary integral methods, or they can be Fourier functions (Dommermuth and Yue, 1987; West *et al*, 1987), or Bessel functions etc. See Tsai and Yue (1996) for a review. Fourier functions have several advantages: The functions and their derivatives are easy to compute, they are nonsingular, a small number of functions yields high accuracy (nearly exponential convergence), and they can be efficiently computed via a fast Fourier transform (FFT). For N grid points, the computational cost is $O(N \log N)$, which is similar to Boussinesq methods and compares favorably to other methods which are typically at least $O(N^2)$. Their apparent disadvantages seem to be: They impose periodicity and the medium is assumed to be homogeneous (constant mean depth).

Most of the methods used are subject to a trade-off between computational efficiency, and dispersivity. Boussinesq methods are efficient, corresponding to sparse algebraic systems, but have limited dispersion. Boundary integral methods use full systems which are computationally demanding. The FFT algorithm enables us to solve certain full systems (Fourier transforms) in an efficient manner, maintaining full dispersivity. In the present work we overcome one apparent disadvantages of Fourier methods in the following way. The boundary value problem is decomposed into a "sum of two problems" – a simple "steady flow" type solution which allows "wave-maker" or radiation conditions to be satisfied at the lateral control surfaces, and a periodic potential

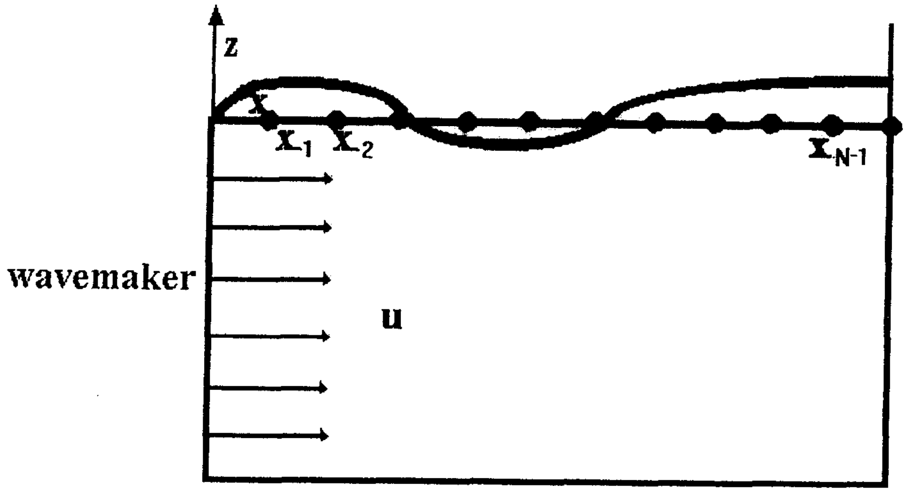

FIGURE 1. Definition sketch

which ensures satisfaction of the free surface and bottom boundary conditions. In this way the accuracy and efficiency of a spectral representation can be enjoyed for spatially non-periodic problems. In the past, the limitation to periodic problems was partially overcome by extending the computational domain until boundary effects essentially disappeared. This involved employing computational domains which were 64 times larger than the physical domain being modeled.

In Section 2 we present the solution to the problem of non-periodic flow fields. An example of nonlinear wave groups evolution is presented in Section 3 and compared to experiments by Shemer *et al* (1998). Conclusions are given in Section 4.

2. Solution of non-periodic problems

Fig. 1 shows a definition sketch of the problem. The coordinate system is taken with the $z = 0$ plane at the mean free surface and the z-axis positive upwards; $\vec{x} = (x, y)$ is defined as a horizontal vector. The flow is assumed to be irrotational, and the fluid incompressible and inviscid; surface tension is neglected. The fluid volume $\mathcal{V}(\vec{x}, z, t)$ is bounded by a free-surface $z = \eta(\vec{x}, t)$ and by a bottom $z = -h(\vec{x})$. We retain a depth variation in the formulation of the problem with an eye to the future, although calculations are only presented here for the constant water depth case. Under the above assumptions the flow can be described by a scalar velocity potential $\phi(\vec{x}, z, t)$ which satisfies the following initial-boundary-value problem.

$$\nabla^2\phi + \phi_{zz} = 0 \qquad \text{in } \mathcal{V} \tag{1}$$

$$\eta_t + \nabla\phi \cdot \nabla\eta - \phi_z = 0 \qquad z = \eta \tag{2}$$

$$\phi_t + \frac{1}{2}(\nabla\phi)^2 + \frac{1}{2}\phi_z^2 + g\eta = 0 \qquad z = \eta$$

$$\phi_z + \nabla\phi \cdot \nabla h = 0 \qquad z = -h \tag{3}$$

$$\phi(\vec{x}, 0, 0) = \eta(\vec{x}, 0) = 0. \tag{4}$$

In the above equations

$$\nabla = (\frac{\partial}{\partial x}, \frac{\partial}{\partial y}), \quad \vec{u} = (u, v) = \nabla\phi, \quad w = \phi_z, \tag{5}$$

In order to use a Fourier-spectral method to solve this problem, the domain $\mathcal{V}$ is enclosed within a set of control surfaces which, for illustration, are taken to be the vertical planes at $x = 0$, $x = L$, $y = 0$, and $y = M$. On these control surfaces, boundary conditions of the following form are applied:

$$\vec{u}_n = \sum_{l=1}^{N_3} c_l \vec{U}_l \tag{6}$$

where N_3 is the total number of degrees of freedom distributed over the control surface, $\vec{u}_n$ is the velocity normal to each control surface b_i; $i = 1, 2, 3, 4$, and the $\vec{U}_l$ are functions of time and of the horizontal coordinate. The $\vec{U}_l$ are chosen to represent a wave-maker/absorber or a matching to another computational domain. In general $\vec{U}_l$ may have a vertical structure, which can be included in the solution. However, in many applications there is no interest in resolving this structure, which is essentially responsible for evanescent modes that decay exponentially away from the boundary. For simplicity, we demonstrate the method for $\vec{U}_l$ that are independent of z.

The velocity potential is decomposed into the following sum of potentials:

$$\phi = \phi_1 + \phi_2 \tag{7}$$

$$\phi_2 = \sum_{l=1}^{N_3} c_l \phi_{2l}. \tag{8}$$

The potentials ϕ_{2l} are chosen to satisfy the Laplace equation, and the boundary conditions on the bottom and control surfaces, Equation (6) and Equation (3). Note that the problem for ϕ_2 is under-determined, making the choice somewhat arbitrary. It is convenient to take ϕ_2 to be quadratic in x, y and z, corresponding to steady flow fields, in which case the consequent horizontal velocity is independent of z. As an example, take ϕ_{21} to be the solution for the two dimensional flow with $u = 0$ on $x = 0$, $y = 0$, and $y = M$; but $u = U(t)$ at $x = L$. This is simply a corner flow, and the solution up to $O(\nabla h)$ is

$$\nabla\phi_{21} = \frac{U}{L}(x - 2(z + h)\nabla h, 0, -(z + h + x\nabla h)). \tag{9}$$

Where on an even bottom ∇h vanishes, yielding:

$$\phi_{21} = \frac{U}{2L}(x^2 - (z + h)^2) \tag{10}$$

Similar solutions can be used for the remaining ϕ_{2l} corresponding to uniform flows through the other three vertical control boundaries. If U has spatial structure over the control surface, $U = U_0(t)f(y, z)$, ϕ_2 can be pre-solved for the lateral boundary conditions, producing a set of time-independent response functions which may then be used in the solution, at each time step.

Having chosen the appropriate form of Equation (6) to account for a wavemaker at one end and ensure the radiation of waves at the other end, for example, the other part of the potential ϕ_1, represents a flow in a closed basin, with a prescribed potential on the free surface.

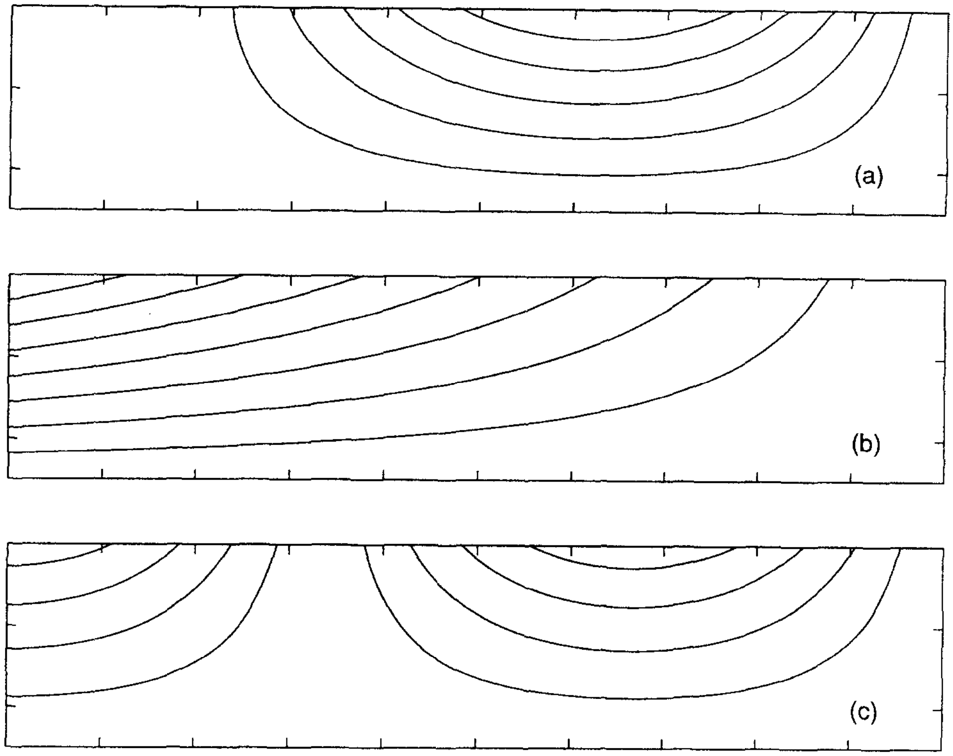

FIGURE 2. Illustration of the components of the potential for a simple wave: (a) Streamlines of ϕ_1, (b) Streamlines of ϕ_2, (c) Streamlines of $\phi_1 + \phi_2$.

We study the case of constant water depth. Since ϕ_1 has zero flux through the boundaries, we may expand it in the following form.

$$\phi_1 = \sum_{m=1}^{N_1} \sum_{n=1}^{N_2} a_{mn} \frac{\cosh k_{mn}(z+h)}{\cosh k_{mn}h} \cos(\vec{k}_{mn} \cdot \vec{x}) \tag{11}$$

$$\nabla\phi_1 = \sum_{m=1}^{N_1} \sum_{n=1}^{N_2} -\vec{k}_{mn}\, a_{mn} \frac{\cosh k_{mn}(z+h)}{\cosh k_{mn}h} \sin(\vec{k}_{mn} \cdot \vec{x}) \tag{12}$$

$$\phi_{1z} = \sum_{m=1}^{N_1} \sum_{n=1}^{N_2} k_{mn}\, a_{mn} \frac{\sinh k_{mn}(z+h)}{\cosh k_{mn}h} \cos(\vec{k}_{mn} \cdot \vec{x}), \tag{13}$$

where

$$\vec{k}_{mn} = (\frac{mL}{\pi}, \frac{nM}{\pi}), \text{ and } \quad k_{mn} = |\vec{k}_{mn}|. \tag{14}$$

The decomposition of the potential is shown schematically in Fig. 2, which sketches the streamlines of each of the flows that correspond to ϕ_1, ϕ_2 and $\phi_1 + \phi_2$, due to a wavemaker on the left end and a reflecting wall at the right end. The complete potential $\phi_1 + \phi_2$ must satisfy the remaining boundary conditions. Upon substituting

Equation (7) into the free-surface conditions we obtain

$$\begin{aligned} \eta_t &= -\nabla(\phi_1+\phi_2)\cdot\nabla\eta + \phi_{1z} + \phi_{2z} \qquad z=\eta \\ \phi_{1t} &= -\phi_{2t} - \frac{1}{2}(\nabla(\phi_1+\phi_2))^2 - \frac{1}{2}(\phi_{1z}+\phi_{2z})^2 - g\eta \qquad z=\eta \end{aligned} \tag{15}$$

as the conditions for ϕ_1.

In order to solve for the evolution of the velocity potential, we need to solve for the evolution of the $N = N_1 \times N_2$ functions $a_{mn}(t)$ and for the N_3 functions ϕ_{2l}. N collocation points are distributed on a regular grid over the free surface. At the free surface points, Equations (7) and (11) through (13) relate a_{mn} to ϕ. The ϕ_{2l} functions are determined from the lateral boundary condition Equation (6), using the pre-solved "steady flows". This completes the solution of Laplace equation. To proceed, Equations (15) are marched in time to find the new time values of ϕ and η. The derivatives of ϕ_2 are known since ϕ_2 is known in functional form. The derivatives of ϕ_1 are given in Equations (12, 13) in terms of the coefficients a_{mn}. This makes the evaluation of the derivatives efficient and accurate. The gradient of η can be derived by finite differences or a variant of the FFT. Since this quantity enters only through nonlinear terms in the free-surface condition, the accuracy of its evaluation can meet lower requirements than those satisfied by the potential. As described above the method is fully nonlinear, and the dominant workload comes from building and inverting an $N \times N$ matrix at every time step; and is thus of $O(N^3)$. The solution in this form represents an extension to non-periodic problems of [2]. As long as an effective means of pre-conditioning can be developed, the resultant linear system can, in principle, be solved iteratively reducing the workload to $O(N^2)$. An alternative, however, is to expand the values of ϕ_1 and its derivatives on the free surface in a Taylor series about the value on the still water level, thus producing a method correct up to some fixed order of nonlinearity, M. In this case, the FFT may be used to reduce the work load to $O(MN\log N)$. The method is described by Dommermuth and Yue (1987) and we briefly review it here.

Let us write ϕ in a perturbation series in the nonlinearity parameter ϵ (which is the order of the wave steepness):

$$\phi = \sum_{i=1}^{M} \phi^{(i)} \tag{16}$$

where $\phi^{(i)} = O(\epsilon^i)$. The value of $\phi^{(i)}$ (and its derivatives) on the free surface ($z=\eta$) can be evaluated from a Taylor series about $z=0$:

$$\phi_{(z=\eta)} = \sum_{i=1}^{M}\sum_{j=0}^{M-i} \frac{\eta^j}{j!}\frac{\partial^j}{\partial z^j}\phi^{(i)}_{(z=0)} \tag{17}$$

(and similar expressions for its derivatives).

Thus, we may use these expressions to march Eq. (2) in time, and obtain the values of η and of $\phi^s = \phi(z=\eta)$ at the following time step. In order to continue the procedure, we then need to find $\phi^{(i)}$ on $z=0$, at the new time step. Collecting terms at each order in Eq. (17), we may evaluate a sequence of equations for $\phi^{(i)}_{(z=0)}$:

$$\phi^{(1)}_{(z=0)} = \phi^s \tag{18}$$

$$\text{and } \phi^{(i)}_{(z=0)} = -\sum_{j=1}^{i-1} \frac{\eta^j}{j!}\frac{\partial^j}{\partial z^j}\phi^{(i-j)}_{(z=0)},\ i = 2,3,...,M. \tag{19}$$

where after evaluating $\phi^{(i)}_{(z=0)}$ at each order, we use a fast cosine transform to determine the coefficients a_{mn}, thus knowing ϕ_1 and its derivatives at $z=0$ in terms of FFT's. We then proceed to the next order in nonlinearity.

3. The evolution of wave groups

In order to demonstrate the performance of the non-periodic High Order Spectral method, we have chosen a relatively simple problem. The evolution of wave-groups (with narrow spectra) on an even bottom has recently been studied experimentally and numerically by Shemer *et al* (1998). The waves are generated at one end of a flume by a wave-maker and propagate along the flume until they are damped at its end. Their nonlinear interaction is studied by recording the waves at a few locations along the flume. Their study addressed the demodulation (or focusing) which occurs within the group. The effect depends on the dispersiveness of the waves, which depends on whether the ratio of wavelength to water depth is larger or smaller than a critical value. When the waves are steeper, this nonlinear evolution is more intense. These features of the wave evolution are successfully predicted by the cubic Schroedinger equation which was used by Shemer *et al* as a model equation. The main aspect which can not be predicted by the cubic Schroedinger equation, due to its structure, is the development of asymmetry in the wave-groups (and the wave spectrum). They suggest some models that can be used in deep water and others which are valid in fairly shallow water (*eg* the Korteveg - de Vries equation.) Here we compare the predictions of the non-periodic spectral model with the measurements of Shemer *et al* for one experiment. Both the focusing and the development of asymmetry are successfully described by the model.

In order to absorb the waves at the end of the flume, it is possible to use an active wave-absorber, which is just a wave-maker. Active wave-absorbers are very efficient in absorbing linear waves. Absorption of nonlinear waves is most effectively done by a combination of active absorption and a damping zone applied to a portion of the free-surface. So far, we have only implemented the damping free surface condition (often referred to as a sponge layer) which requires an extended computational domain. Present day sponge layers require about a full wavelength for effective absorption. Work on an improved sponge layer is in progress.

The characteristics of the waves studied are as follows: Water depth: $h = 60$ cm; peak wave period: $T = 0.7$ s. This corresponds to a peak wavenumber: $k = 8.21$ m^{-1}. The wave-maker stroke is given by:

$$s = s_0 \exp(-t/5T)^2) \cos(2\pi t/T)$$

where $-16T < t < 16T$. The maximum wave steepness at $x = 0.24$ m is $ka_{max} = 0.246$, where $a_{max} = (\eta_{peak} + \eta_{trough})/2$. The computational wave-maker was matched to the experiments by adjusting s_0 to obtain the correct ka_{max} at $x = 0.24$ m. In Fig. 3 are shown the measured and the computed time records of the surface elevation, at the locations: $x = 0.24$ m and $x = 8.67$ m. We see that the model faithfully captures the focusing of wave energy as well as the onset and growth of asymmetry in the waveform. The measurements were taken after many wave periods, after a quasi-steady state has been reached. The computations results are plotted shortly after the motion started. This avoided the appearance of small reflected waves, which should be eliminated by improved absorption.

4. Conclusions

A method for the solution of non-periodic problems by a pseudo-spectral technique has been developed and demonstrated for water waves. The method is based on writing the potential as a superposition of a component that is chosen to satisfy the lateral boundary conditions and a spatially periodic component, with no flux through the lateral boundaries. The latter is computed most efficiently through the FFT algorithm.

The efficiency of the method makes it an attractive tool for the study of complex problems. It can also be used for the intensive computations required for Monte-Carlo simulations of stochastic problems. Further extension of the High Order Spectral method to a topography with large depth variations is the next important step in its development.

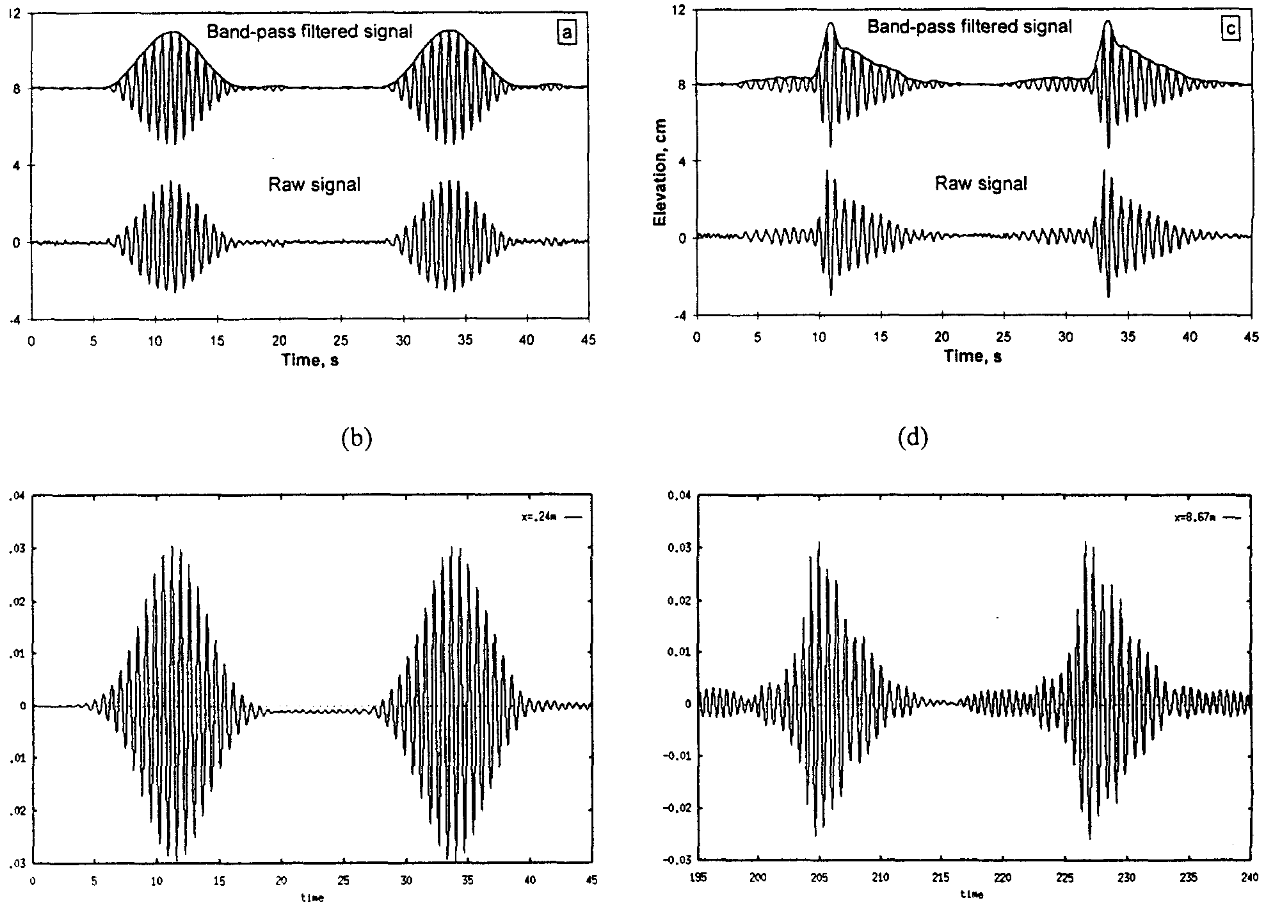

FIGURE 3. (a) The measured wave elevation at $x = 0.24$ m. (b) The computed wave elevation at $x = 0.24$ m. (c) The measured wave elevation at $x = 8.67$ m. (d) The computed wave elevation at $x = 8.67$ m.

Acknowledgements

We thank Profs. Lev Shemer and Eliezer Kit from Tel-Aviv University for kindly providing us with their experimental results. This research was supported by the Danish National Research Foundation. Their support is greatly appreciated.

References

[1] Dommermuth D.G., Yue D.K.P., 1987. A high-order spectral method for the study of nonlinear gravity waves, *J. Fluid Mech.* **184**, 267-288.

[2] Fenton J.D., Rienecker M.M., 1982. A Fourier method for solving nonlinear water-wave problems: application to solitary-wave interactions, *J. Fluid Mech.* **118**, 411-443.
[3] Madsen P.A., Schäffer H.A., 1998. Higher order Boussinesq-type equations for surface gravity waves - derivation and analysis. *Phil. Trans. R. Soc.*, Series A, London, **356**, 3123-3184.
[4] Shemer L., Kit E., Jiao Hai Ying, Eitan O., 1998. Experiments on nonlinear wave groups in intermediate water depth. *Journal of Waterway Port Coastal and Ocean Engineering - ASCE*, **124:(6)**, 320-327.
[5] Tsai W., Yue D.K.P., 1996. Computation of nonlinear free-surface flows. *Annu. Rev. Fluid. Mech.*, **28**, 249-278.
[6] West B. J., Brueckner K.A., Janda R.S., Milder M., Milton R.L., 1987. A new numerical method for surface hydrodynamics. *J. Geophys. Res.* **92**, 11, 803-824.